MOLECULAR AND CELLULAR BIOLOGY, Feb. 2000, p. 1124–1133 Vol. 20, No. 4
0270-7306/00/$04.00+0

The Orphan Nuclear Receptor SHP Utilizes Conserved LXXLL-Related Motifs for Interactions with Ligand-Activated Estrogen Receptors

LOTTA JOHANSSON,[1] ANN BÅVNER,[1] JANE S. THOMSEN,[1] MATHIAS FÄRNEGÅRDH,[2] JAN-ÅKE GUSTAFSSON,[1] AND ECKARDT TREUTER[1]*

Department of Biosciences at Novum, Karolinska Institute,[1] and KaroBio AB,[2] S-14157 Huddinge, Sweden

Received 16 July 1999/Returned for modification 24 August 1999/Accepted 11 November 1999

SHP (short heterodimer partner) is an unusual orphan nuclear receptor consisting only of a ligand-binding domain, and it exhibits unique features of interaction with conventional nuclear receptors. While the mechanistic basis of these interactions has remained enigmatic, SHP has been suggested to inhibit nuclear receptor activation by at least three alternatives; inhibition of DNA binding via dimerization, direct antagonism of coactivator function via competition, and possibly transrepression via recruitment of putative corepressors. We now show that SHP binds directly to estrogen receptors via LXXLL-related motifs. Similar motifs, referred to as NR (nuclear receptor) boxes, are usually critical for the binding of coactivators to the ligand-regulated activation domain AF-2 within nuclear receptors. In concordance with the NR box dependency, SHP requires the intact AF-2 domain of agonist-bound estrogen receptors for interaction. Mutations within the ligand-binding domain helix 12, or binding of antagonistic ligands, which are known to result in an incomplete AF-2 surface, abolish interactions with SHP. Supporting the idea that SHP directly antagonizes receptor activation via AF-2 binding, we demonstrate that SHP variants, carrying either interaction-defective NR box mutations or a deletion of the repressor domain, have lost the capacity to inhibit agonist-dependent transcriptional estrogen receptor activation. Furthermore, our studies indicate that SHP may function as a cofactor via the formation of ternary complexes with dimeric receptors on DNA. These novel insights provide a mechanistic explanation for the inhibitory role of SHP in nuclear receptor signaling, and they may explain how SHP functions as a negative coregulator or corepressor for ligand-activated receptors, a novel and unique function for an orphan nuclear receptor.

Nuclear receptors (NRs) are modular eucaryotic transcription factors that usually are comprised of two functionally independent and conserved domains (9, 24). A conserved DNA-binding domain (DBD) allows them to associate directly with specific DNA response elements. A ligand-binding domain (LBD) is required for the binding of small lipophilic molecules, ligands or hormones, and for the transmission of ligand signals to transcriptional responses. Ligands have not been identified or may not exist for all family members (orphan receptors), and alternative ligand-independent signaling pathways for transcriptional activation have been suggested (9, 24). In case of ligand signaling, conformational changes within the LBD are essential for the transmission process via a ligand-regulatable activation domain, AF-2. In particular, the structural configuration of a C-terminal helix 12 has been recognized to be crucial for cofactor recruitment (4, 38, 45). Notably, the majority of the transcriptional cofactors identified primarily target the AF-2 LBD. Critical corepressors such as N-CoR/SMRT may link unliganded receptors to histone deacetylation and chromatin repression (reference 27 and references therein), while critical coactivators such as p160/SRC family members and CREB-binding protein/p300 may link liganded receptors to histone acetylation and chromatin derepression (references 12, 27, 39, and 44 and references therein). Additionally, novel LBD cofactors such as TRAP220/DRIP205 may link receptors to the TRAP-SMCC-DRIP-ARC-CRSP coactivator complex (10, 15, 42), which appears to act in an acetylation-independent manner directly on the basal transcription machinery. Other putative cofactors have been isolated, including RIP140 and NSD1 (5, 14, 41), whose function in NR signaling remains unclear and which do not simply act as coactivators or corepressors.

Two-hybrid interaction screenings aimed in identifying novel cofactors for the LBD of NRs have led to the identification of an unusual orphan NR consisting only of a putative LBD (16, 25, 35). Based on its ability to interact with a variety of NRs, it has been termed SHP (short heterodimer partner; also called NROB2 [1]); however, distinct features distinguishes SHP from retinoid X receptor (RXR), the only known common heterodimerization receptor. First, SHP, unlike RXR, interacts with estrogen receptors (ERs) and agonistic ligands enhance whereas antagonistic ligands inhibit these interactions (for discussions, see references 16 and 37). Second, the entire C terminus within SHP, including the putative dimerization helix, is dispensable for interactions, and a central LBD region apparently forms the SHP-specific domain for interaction with receptors. SHP has been suggested to play a very general negative role in NR signaling. For example, in transient transfections, SHP inhibits transcriptional activation of its receptor targets, an inhibition which may be further potentiated due to the presence of an intrinsic transcriptional repression domain. In vitro, SHP has been shown to inhibit binding of retinoic acid receptor-RXR heterodimers to DNA response elements, suggesting that competitive dimerization may result in novel SHP heterodimers that are unable to bind DNA. Based on our recent studies on SHP and ERs (16), we have proposed a novel inhibitory mechanism for SHP. We have demonstrated that

* Corresponding author. Mailing address: Department of Biosciences at Novum, Karolinska Institute, S-14157 Huddinge, Sweden. Phone: 46 8 608 9160. Fax: 46 8 774 5538. E-mail: eckardt.treuter@csb.ki.se.

SHP and AF-2 coactivators such as TIF2 directly compete for binding to ERs, suggesting either that SHP and AF-2 coactivators contact a common surface or, alternatively, that binding of SHP to the LBD induces conformational changes that cause the dissociation of AF-2 coactivators.

In this study, we have identified two functional AF-2-binding motifs within SHP which critically determine the interaction of SHP with ERs. The SHP motifs closely resemble the LXXLL motifs, referred to as NR boxes or LCD/LXD motifs (13, 20, 40), which are characteristic for most AF-2 coactivators and coregulators. Functional studies and three-dimensional structures of various LBDs in complex with peptides or coactivator fragments indicate that the LXXLL core directly binds the AF-2 domain. This domain consists of a hydrophobic binding groove on the surface of the LBD formed by residues from helices 3 to 5, also known as the static region or signature region, and helix 12, also known as the flexible region or AF-2 AD. Consistent with the functional conservation of ligand activation mediated by specified coactivators, these residues are highly conserved between all ligand-activatable receptors including the two ER subtypes (references 7, 23, and 38 and references therein).

The unanticipated existence of functional NR boxes within the putative SHP LBD suggests that SHP mimics the interaction of NR-associated transcriptional cofactors, a unique function for a member of the NR superfamily. The results of this study provide the mechanistic explanation for previously less understood interaction characteristics of SHP and allow envisaging how SHP, independently of DNA-binding and conventional dimerization-type interactions, might exert its inhibitory effect on NRs.

MATERIALS AND METHODS

Plasmids. All plasmids were generated using standard cloning procedures and verified by DNA sequencing.

(i) Yeast expression plasmids. The Gal4 activation domain (GalAD) fusion constructs GalAD-human ERα (hERα) LBD/AF2 (amino acids [aa] 249 to 595) and GalAD-rat ERβ (rERβ) LBD/AF2 (aa 168 to 485) were constructed by inserting PCR-generated fragments of the corresponding ER cDNAs (31) into the *Bam*HI site of pACT2 (Clontech). The Gal4 DBD fusion construct Gal4–wild-type SHP (SHPwt) (aa 1 to 260) was made by cloning a PCR-generated fragment of rat SHP cDNA into the *Eco*RI/*Bam*HI sites of pAS2-1 (Clontech). Point mutations were introduced into the SHP sequence by PCR-mediated mutagenesis using primers containing the different mutations. The mutated inserts were cloned into the *Eco*RI/*Bam*HI site of pAS2-1. Gal4-SHP box 2 peptide (aa 116 to 129) and Gal4-TIF2 box 2 peptide (aa 687 to 700) constructs were made by inserting the corresponding double-stranded oligonucleotide into the *Eco*RI/*Sa*l sites of pAS2-1.

(ii) GST-His fusion constructs. Glutathione *S*-transferase (GST)–mouse ERα (mERα) LBD/AF2 (aa 313 to 595) and GST-mERα LBD/AF2 M547A/L548A (aa 313 to 595) have been described before (5). GST-SHP box 2 peptide and GST-TIF2 box 2 peptide were constructed by inserting the corresponding double-stranded oligonucleotide (see above) into the *Eco*RI/*Sa*l sites of pGEX4T-1. The His-SHPwt (aa 1 to 260) and the GST-SHPwt (aa 1 to 260) constructs have been described previously (16).

(iii) Plasmids for in vitro translation. pT7hERα (aa 1 to 595), pBKCMV HA hERβ (aa 1 to 485), and pBKCMV HA TIF2 (aa 1 to 1465) have been described previously (reference 16 and references therein). pSG5 SHPwt (aa 1 to 260) was constructed by using the same PCR fragments as for the yeast vectors inserted into the *Eco*RI/*Bam*HI sites of pSG5 (Stratagene). The different point mutations of SHP were also constructed by using the same PCR fragments as for the yeast vectors inserted into the *Eco*RI/*Bam*HI sites of pSG5. pGEMThERβ L490A/L491A was generated by site-directed mutagenesis, and phERα L540A/L541A has been described before (30). pBKCMV HA TIF2 (aa 596 to 766) has also been described previously (21).

(iv) Mammalian expression constructs. pSG5-based expression vectors for hERα and hERβ (31) and the ER reporter construct 3xERE-TATA-luc have been described previously (17). pcDNA3 VP16 was made by inserting VP16 as a *Bam*HI/*Xho*I fragment into pcDNA3 (Invitrogen). pcDNA VP16-SHPN1 (aa 37 to 260) was generated by inserting the corresponding PCR fragment into the *Eco*RI site of pcDNA3 VP16. pcDNA VP16-TIF2 (aa 596 to 766) was generated by cloning an *Eco*RI/*Xho*I fragment from pBKCMV HA TIF2. pSG5 SHP159 (aa 1 to 159) was generated by inserting the corresponding PCR fragment containing a nuclear localization signal, PKKKRKV, adjacent to aa 159, to ensure nuclear localization, into the *Eco*RI site of pSG5. More details concerning the constructs are available on request.

Yeast two-hybrid interaction assay. For the yeast interaction assay, *Saccharomyces cerevisiae* HF7c (*MAT***a**) transformed with Gal4 plasmids was mated with strain Y187 (*MAT*α) transformed with GalAD plasmids. Diploid strains were selected for the presence of both plasmids and grown in selective media in the absence (dimethyl sulfoxide) or presence of 1 μM 17β-estradiol (E_2). Interactions were monitored as β-galactosidase (β-Gal) activity in each yeast culture lysate. The values shown are the mean of at least three independent experiments.

GST pull-down assay. Interaction studies were performed essentially as described before (16). Briefly, ^{35}S-labeled proteins, generated by in vitro transcription-translation of either plasmids or PCR products using a TNT kit (Promega), were incubated with approximately 1 μg of GST fusion protein in the absence (DMSO) or presence of 1 μM E_2. The proteins were incubated for 2 h at 4°C. After washing, protein interactions were analyzed by sodium dodecyl sulfate-polyacrylamide gel electrophoresis (SDS-PAGE) followed by autoradiography.

DNA-dependent protein-protein interaction assay. The ability of SHP to interact with DNA-bound ERβ was tested essentially as described by Kurokawa et al. (18). One microgram of double-stranded biotinylated oligonucleotide containing the estrogen response element (ERE) from the vitelogenin A2 gene was incubated with approximately 100 ng of ERβ purified from baculovirus extract. The complex was immobilized on streptavidin Magnesphere paramagnatic beads (Promega) and used to analyze binding of ^{35}S-labeled proteins or whole-cell extracts transiently expressing SHPwt, in the absence or presence of 1 μM E_2 or 1 μM 4-OH tamoxifen (4-OHT). After washing, the complex was resolved by SDS-PAGE and detected by autoradiography. To detect SHPwt protein from cell extracts, the complex was separated by SDS-PAGE, transferred to a nitrocellulose filter, and subjected to Western analysis using the anti-SHP serum. The amount of ERβ bound to the ERE was measured using an affinity-purified rabbit polyclonal ERβ antibody raised against the N terminus of hERβ (a gift from S. Windahl). The ERβ antibody was diluted 1:1,000.

Mammalian cell transfections. 293 human embryo kidney cells were maintained in a 1:1 mixture of F-12 medium with glutamine and Dulbecco's modified Eagle's medium supplemented with 10% fetal calf serum penicillin (100 μl/ml), and streptomycin (100 μl/ml) (Life Technologies, Inc.). Transfections were performed as previously described (16), using phenol red-free medium in the absence (DMSO) or presence of 10 nM E_2 for 24 h. For the SHP mutation study, 0.2 μg of pSG5 ERα or pSG5 ERβ, 0.8 μg of 3xERE-TATA-luc reporter plasmid, and 1 μg of either pSG SHPwt, pSG5 SHPmt1.2, pSG5 SHP159, or pSG5 (empty vector) were used per 35-mm-diameter well. For the one-hybrid study, 10 ng of pSG5 ERα or 0.1 μg of pSG5 ERβ was used together with increasing amounts of pcDNA VP16-SHPN1 or pcDNA VP16-TIF2. pcDNA VP16 was added to equalize total transfected plasmid DNA concentrations. Cos7 monkey kidney cells, used for preparing whole-cell extracts, were maintained in Dulbecco's modified Eagle medium supplemented with 10% fetal calf serum, penicillin (100 μl/ml), and streptomycin (100 μl/ml), plated on 100-mm-diameter plates, and transfected with 4 μg of pSG5 SHPwt, pSG5 SHPmt1.2, or pSG5 SHP159 expression plasmid.

Antibody production and Western analysis. Purified His-tagged SHP protein (aa 1 to 260) was used to immunize rabbits (Zeneca). Antibody specificity was tested using recombinant proteins and whole-cell extracts and also by using depleted serum. For Western analysis of mammalian cells, whole-cell extracts were prepared using a high-salt buffer (10 mM HEPES-KOH [pH 7.9], 0.4 M NaCl, 0.1 mM EDTA, 5% glycerol, 1 mM dithiothreitol, 0.5 mM phenylmethylsulfonyl fluoride), separated by SDS-PAGE, and transferred onto a nitrocellulose filter (Amersham Pharmacia Biotech). Filters were blocked with 5% milk powder in PBS-Tween 20 and incubated with 1:1,000 dilution of anti-SHP serum in PBS-Tween 20 plus 5% milk powder for 2 h at room temperature. After washing the filters were incubated with horseradish peroxidase-conjugated secondary anti-immunoglobulin G antibody (Amersham Pharmacia Biotech) at a dilution of 1:12,000 in PBS-Tween 20 plus 5% milk powder for 2 h at room temperature. After washing, the proteins were visualized with X-ray film using an enhanced chemiluminescence system (Amersham Pharmacia Biotech). For Western analysis of yeast cells, whole-cell extracts of the same diploid strains used for the β-Gal assay were prepared according to the recommended protocol (Clontech), and the Western analysis was performed as described above, using a 1:2,000 dilution of a mouse monoclonal antibody raised against the Gal4 DBD (RK5C1; Santa Cruz Biotechnology).

RESULTS

Identification of NR box motifs within SHP and involvement of these motifs in interaction with ERs. Based on striking similarities between SHP and AF-2 cofactors, such as the coactivator TIF2, in their interaction characteristics with ERs (16), we scrutinized the previously identified minimal receptor interaction domain in the central part of SHP (aa 92 to 148) (36, 37) and surprisingly identified an NR box-like motif with the core sequence LXXIL (referred to below as box 2). This

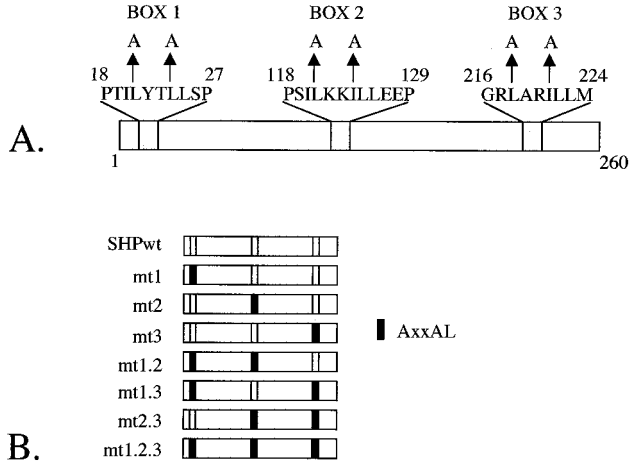

FIG. 1. (A) Schematic picture of the SHP protein, showing the sequences and locations of the three putative NR boxes. Arrows show the amino acids changed to alanine. (B) Illustration of the different constructs used. The mutated boxes are in black. The mutants are named after the mutated boxes.

finding gave rise to the intriguing possibility that the interactions of the central SHP domain with receptors are determined through this motif. When investigating the entire sequence, we found that SHP contains two additional related motifs (Fig. 1A; see also Fig. 8). One motif (referred to below as box 1) is located within the N-terminal part of SHP; the other motif (referred to below as box 3) is located within the C-terminal part of the LBD, which in NRs usually encompasses the dimerization domain helix 10/11 (45).

To investigate the involvement of these three motifs in the interactions of SHP with ERs, we made a series of NR box mutants. Alanine substitutions were introduced in the critical NR box core positions +1 and +4 (LXXI/LL to AXXAL), in the context of the full-length SHP, either alone or in a combination with two or three of the boxes (Fig. 1B). The different mutants were studied according to their interaction potential with human ERα and -β in comparison with SHPwt, both in vitro, using GST pull-downs (Fig. 2A), and in vivo, using the yeast two-hybrid system (Fig. 2B and C). In the GST pull-down assay, ^{35}S-labeled SHP (wild type or mutants) was used together with GST-ERα. Whereas the in vitro interaction between ERα and SHPwt was strongly dependent on the presence of E_2 (Fig. 2A, compare lanes 3 and 4) as shown before (16, 37), the triple mutation SHPmt1.2.3 completely abolished the interaction with ERα (Fig. 2A, lanes 31 and 32). In addition, the double mutation of box 1 and box 2, leaving box 3 intact, completely abrogated the interaction with ERα (Fig. 2A, lanes 19 and 20). In contrast, none of the single mutations abolished the interaction (Fig. 2A, lanes 8, 12, and 16). These results were confirmed in the yeast two-hybrid assay using GalAD-ERα or GalAD-ERβ together with Gal4-SHP (wild type or mutants). The triple mutant, as well as the double mutation of boxes 1 and 2, abolished the ligand-dependent

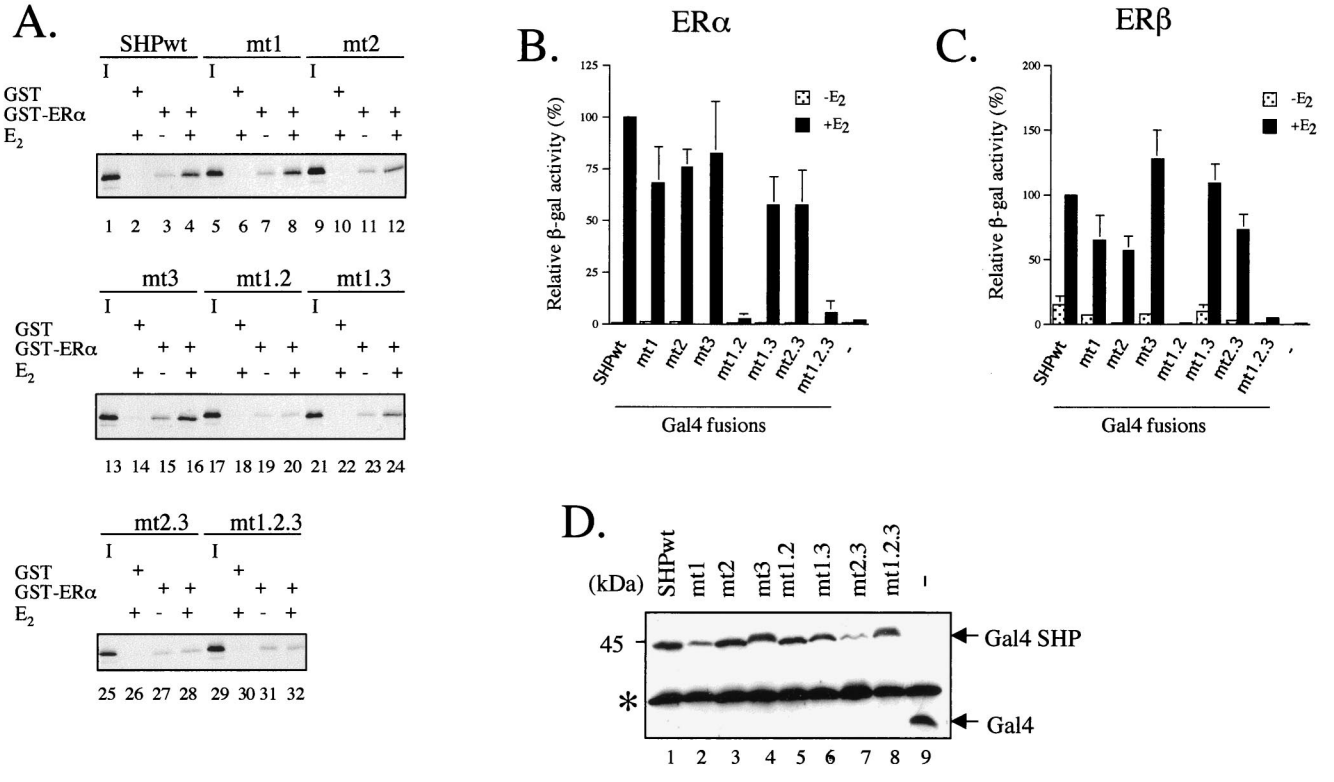

FIG. 2. The interaction of SHP with ERα and ERβ is dependent on the integrity of NR box motifs within SHP. (A) In vitro interaction between SHP and ERα. The different SHP mutants were ^{35}S labeled and analyzed in a pull-down assay using purified GST-ERα (aa 313 to 595) or GST alone in the absence or presence of 1 μM E_2. The approximated size of SHP is 30 kDa. The input represents 10% of the amount of labeled protein used in each pull-down. (B and C) Yeast two-hybrid interaction between SHP and ERs. HF7c, containing the different Gal4-SHP fusions, was mated to Y187 containing either GalAD-ERα (aa 249 to 595) (B) or GalAD-ERβ (aa 168 to 485) (C) β-gal activity was measured in the absence or presence of 1μM E_2. The β-Gal activity observed with SHPwt in the presence of E_2 was set to 100%. Values shown are the means of three independent experiments. (D) Western blot showing expression of the different Gal4-SHP fusions in yeast, using a Gal4 DBD antibody. The approximated size of Gal4-SHP is 45 kDa. * represents an unspecific band present in all samples.

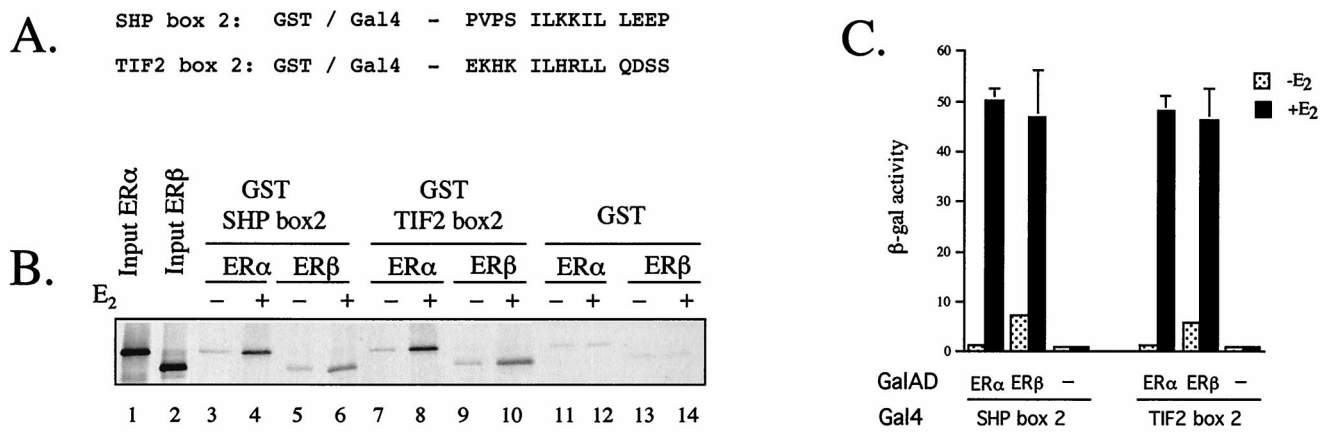

FIG. 3. The SHP NR box 2 motif is sufficient for ligand-dependent interaction with ERα and ERβ. (A) Sequences of the two peptides, SHP NR box 2 and TIF2 NR box 2, fused to either GST or Gal4. (B) Pull-down assay using ^{35}S-labeled wild-type ERα or ERβ together with purified GST-SHP NR box 2, GST-TIF2 NR box 2, or GST alone in the absence or presence of 1 μM E_2. The approximated size of ERα is 67 kDa, and that of ERβ is 60 kDa. The input represents 10% of the amount of labeled protein used in each pull-down. (C) Yeast two-hybrid interactions between ERs and SHP NR box 2 and TIF2 NR box 2. HF7c containing the Gal4-SHP NR box 2 or Gal4-TIF2 NR box 2 construct was mated to Y187 containing either GalAD-ERα (aa 249 to 595) or GalAD-ERβ (aa 168 to 485). β-Gal activity was measured in the absence or presence of 1 μM E_2. Values shown are the means of three independent experiments.

interaction of SHP with both ERα and ERβ (Fig. 2B and C). That a combined mutation of boxes 1 and 2 leads to loss of receptor interaction was similarly observed with both thyroid hormone receptor and RXR, indicating that the two SHP NR boxes may also specify the interactions with other NRs (data not shown). Importantly, all of the different SHP fusion proteins were expressed in yeast (Fig. 2D). The finding that the loss of receptor interaction occurred with the double mutation of boxes 1 and 2, still containing an intact box 3, suggests that the putative dimerization surface of SHP (see Fig. 8) is not involved in interaction with NRs. Furthermore, boxes 1 and 2 seem to be functionally redundant since the mutation of a single box is not sufficient to abolish interaction with ERs. In summary, we conclude from these experiments that boxes 1 and 2, but not box 3, can function as interaction motifs which are necessary for the interaction with the ERs both in vitro and in vivo.

The SHP NR box 2 motif is sufficient for ligand-dependent interaction with ERα and -β. To rule out indirect effects of the NR box mutations on adjacent putative interaction surfaces and to analyze whether interactions of the previously identified central ER interaction domain (37) were mediated by the internal SHP box 2 motif, we examined whether this motif was sufficient for interaction. Recent studies have demonstrated functionality of short peptide motifs in the case of other NR box core sequences (7, 8, 13), and thus a peptide containing the SHP NR box 2 motif was fused to either GST or Gal4 (Fig. 3A) and used in either GST pull-downs or the yeast two-hybrid assay. As an important specificity control, we included in our study a peptide containing the TIF2 (GRIP1) NR box 2 motif for the following reasons: (i) it is reported to have the highest affinity for ERα among the three p160 NR boxes (26), (ii) the three-dimensional structure of an identical GRIP1 peptide bound to the LBD of ERα has been determined (38), and (iii) we have previously shown that SHP and TIF2 efficiently compete for binding to ERs, suggesting comparable affinities and interaction surfaces (16). In the GST pull-down, ERα and ERβ were ^{35}S labeled and the binding to GST-SHP NR box 2 was assessed. Interestingly, SHP NR box 2 was able to interact with both ERα and ERβ in a ligand-dependent manner (Fig. 3B, lanes 3 to 6). This ligand-dependent interaction was also seen with the GST-TIF2 NR box 2 peptide (Fig. 3B, lanes 7 to 10). No interaction was seen with GST alone. These results were supported from data obtained in the yeast two-hybrid assay. SHP NR box 2 peptide fused to Gal4 interacted ligand dependently with both ERα and ERβ (Fig. 3C), as did the TIF2 NR box 2 peptide. Notably, under these conditions SHP and TIF2 boxes interacted equally well with both ERs, reflecting the similarities between SHP and TIF2 with respect to NR interaction. This finding is important considering that similar approaches using ERα previously have suggested significant differences in affinity between NR box peptides derived from relevant cofactors (13) and is in good agreement with quantitative measurements using the corresponding domains or entire proteins (28, 46). We conclude that the SHP box 2 motif has a high affinity for ERs, comparable to that of the high-affinity TIF2 box 2 motif, which is in accord with the competition observed between SHP and TIF2 (16).

AF-2 helix 12 mutations in ERα and ERβ abolish the interaction with SHP. The homology and functionality of the critical SHP motifs box 1 and 2 to LXXLL motifs suggested the AF-2 domain as the primary docking site also for the SHP motifs. To validate this idea, we used ERα and ERβ AF-2 helix 12 mutations, which are predicted to result in an incomplete LXXLL binding surface and are known to abolish NR box-mediated interactions with coactivators (e.g., TIF2 and SRC-1) without affecting dimerization or ligand binding (5, 43). GST-ERα M547A/L548A was used together with ^{35}S-labeled SHPwt, TIF2wt, or ERαwt. As seen in Fig. 4A, lanes 7 to 10, neither SHPwt nor TIF2wt interacted with the AF-2 (helix 12 mutation, whereas the dimerization with ERαwt was unaffected (Fig. 4A, lanes 11 and 12). As a control, both SHP and TIF2 interacted ligand dependently with GST-ERαwt as expected (Fig. 4A, lanes 13 to 16). The necessity of a functional AF-2 for the interaction with SHP has also been seen in the reversed orientation using ^{35}S-labeled ERα L540A/L541A or ERβ L490A/L491A together with GST-SHPwt (Fig. 4B, lanes 8 to 10 and 18 to 20). We conclude that an intact ER AF-2 helix 12 surface is necessary for the interactions with SHP. This is consistent with the fact that all SHP-interacting receptors contain a conserved helix 12 motif, and it clearly indicates the AF-2 domain as the direct interaction surface for SHP.

Functional NR box motifs together with the putative repression domain of SHP are required for SHP to exert its inhibi-

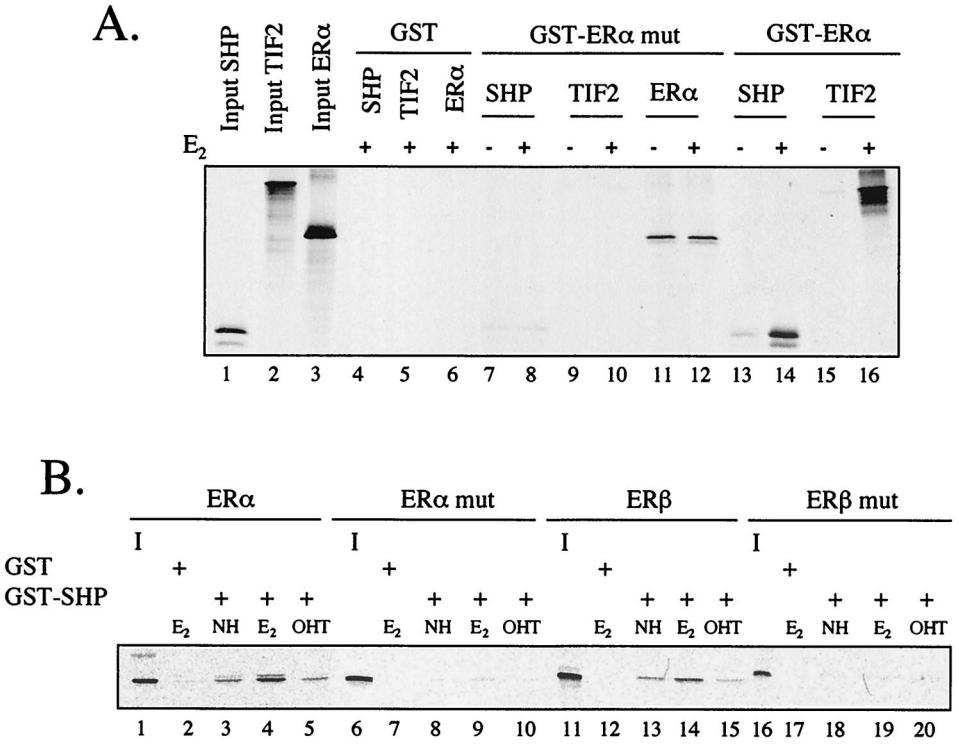

FIG. 4. A functional AF-2 domain of ER is necessary for the interaction with SHP. (A) Wild-type SHP, TIF2, or ERα was ^{35}S labeled and incubated with either GST-ERα M547A/L548A (aa 313 to 595) or GST-ERα (aa 313 to 595) in a pull-down assay in the absence or presence of 1 μM E_2. (B) ERαwt, ERα L540A/L541A, ERβwt, or ERβ L490A/L491A was ^{35}S labeled and incubated with GST-SHP (aa 1 to 260) in the absence or presence of 1 μM E_2 or 1 μM 4-OHT. The input represents 10% of the amount of labeled protein used in each pull-down. Mut, mutant. NH, no hormone.

tory effect on the ligand-dependent activation of ERs. We and others have previously shown that SHP inhibits both ERα and ERβ ligand-induced transactivation in transient transfections (16, 37). In light of the intrinsic repression potential of SHP (36), we wanted to investigate whether inhibition was due to direct interaction of SHP with the ER AF-2 domain via its NR boxes and if this interaction was sufficient for the inhibitory effect of SHP. Studies by Seol et al. (36) have revealed that the SHP construct containing aa 1 to 159 (SHP159) has lost the intrinsic repression activity. SHP159 still contains both NR box 1 and NR box 2 and interacts ligand dependently with both ERα and ERβ in GST pull-downs (reference 36 and data not shown). 293 human embryo kidney cells were transfected using expression vectors for wild-type ERs together with an ER-responsive reporter plasmid. As shown in Fig. 5A and B, coexpression of SHPwt inhibited the ligand-induced transcriptional activity of both ERs. In contrast, coexpression of either the interaction-deficient SHPmt1.2 or the SHP159 did not lead to any inhibition of either ERα or ERβ ligand-induced activity. Similar results were observed for the triple mutant (data not shown). Control Western blot analysis shows that SHPwt, SHPmt1.2, and SHP159 were expressed at comparable levels (Fig. 5C). We therefore conclude that lack of inhibition was not due to decreased stability of the SHP mutants. Additionally, localization studies using GFP fusion proteins demonstrate the presence of SHPwt, SHPmt1.2, and SHP159 in the nucleus, all exhibiting the same dot-like pattern (reference 16 and data not shown). These experiments confirm our model that inhibition requires direct interaction of SHP with the ER AF-2 surface, but they also indicate that the repression domain is necessary for efficacious inhibition.

SHP interacts with the ER dimer on DNA; evidence for ternary complex formation. If SHP, as we suggest, binds exclusively to the AF-2 domain, dimerization or DNA binding of ERs should not be impaired, and ternary complex formation with receptor dimers should be possible. As seen in the crystal structure of ERα (4, 27), AF-2 is available for NR box interactions also in the ER dimer, while the ER dimerization helix 10 is occupied and not accessible for secondary interactions. Indirect evidence has supported this idea, because in vitro-translated SHP did not inhibit DNA binding of ERs in standard band shift assays (reference 37 and data not shown), and SHP did not interfere with ER dimerization in solution (16). To address this important issue, we used two different approaches to detect ternary complex formation. In vitro, we utilized a DNA-dependent protein-protein assay which has been widely used to monitor coactivator interactions with receptor dimers on DNA (18, 22, 42); in vivo, we carried out a modification of the mammalian two-hybrid/coactivation assay using VP16-SHP together with the wild-type ERs.

In the DNA-dependent protein-protein interaction assay, ERβ dimers from baculovirus extract were assembled on biotinylated EREs, immobilized on streptavidin beads, and incubated with either ^{35}S-labeled SHPwt (Fig. 6A), overexpressed SHPwt from Cos7 cells (Fig. 6B), ^{35}S-labeled TIF2 (aa 596 to 766) (Fig. 6C), or ^{35}S-labeled SHPmt1.2 (Fig. 6D). Consistent with the ligand effect seen in solution, SHP interacted with the DNA-bound ERβ dimer in the presence of the agonist E_2 but not in the presence of the antagonist 4-OHT or in the absence of ligand. This was observed using SHP protein from two different sources, i.e., in vitro-translated SHPwt and overexpressed SHPwt from Cos7 cells. For comparison, in vitro-

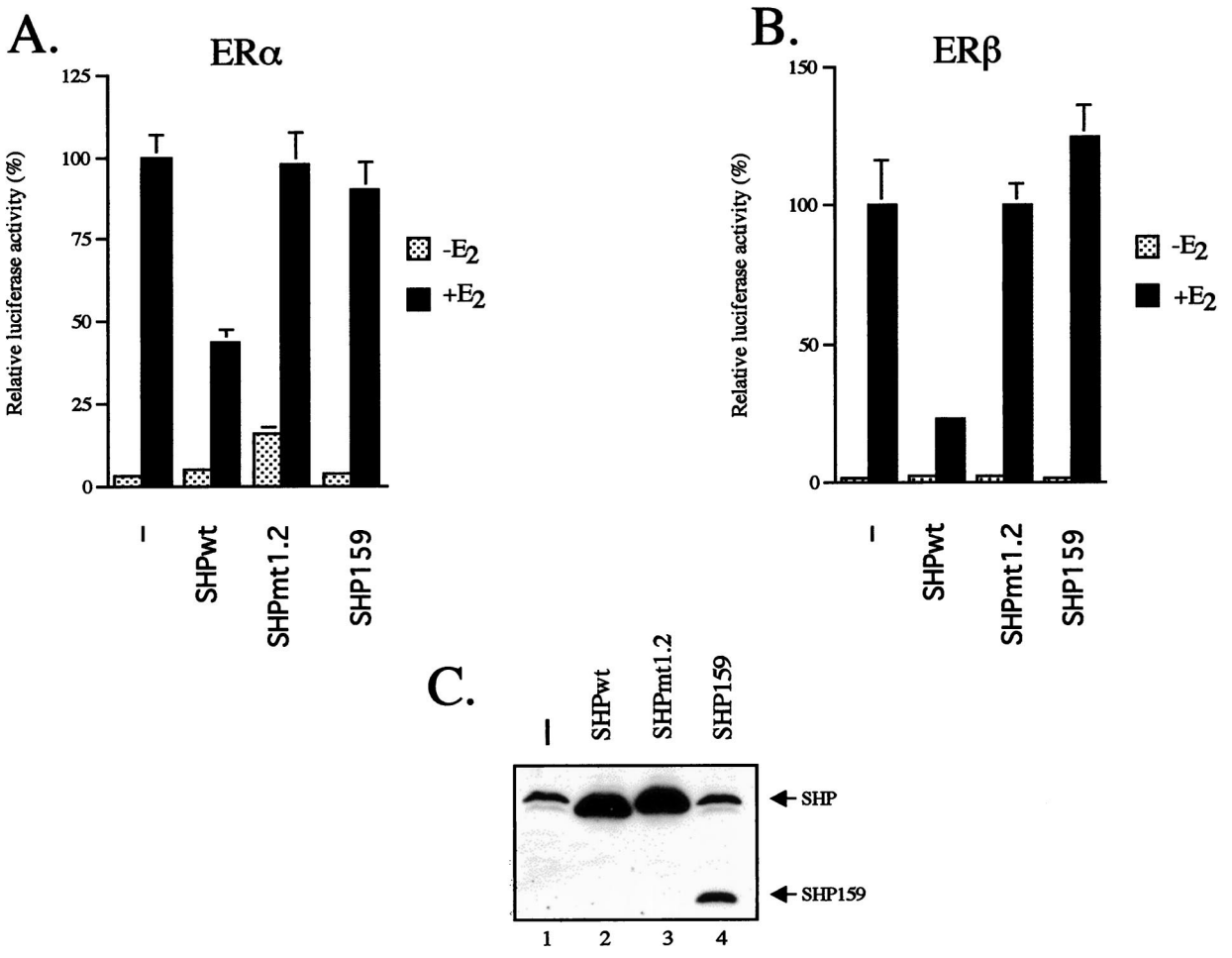

FIG. 5. A direct interaction is necessary but not sufficient for the inhibitory effect of SHP on the ligand-dependent activation of ERs. 293 cells were cotransfected with the ERE-TATA-luc reporter plasmid and the expression plasmids for either ERαwt (A) or ERβwt (B), together with an expression vector for SHPwt, SHPmt1.2, or SHP159, in the absence or presence of 10 nM E_2. Values shown are the means of three independent experiments. (C) Western blot analysis of either nontransfected cells or cells overexpressing SHPwt, SHPmt1.2, or SHP159, using rabbit anti-SHP serum (see Materials and Methods). The approximated size of SHP is 30 kDa. The background band seen in lanes 1 and 4 probably corresponds to endogenous SHP, since this band does not occur when depleted serum is used in a control experiment (data not shown).

translated TIF2 interacted with DNA-bound ERβ dimer in an agonistic-dependent manner, similar to SHP under identical conditions. As expected from our binding assays in solution, SHPmt1.2 was not able to interact with ERβ, irrespective of ligand status. The same results were obtained for ERα (data not shown). Importantly, as judged from the Western controls, binding of ER to DNA took place regardless of ligand status and of SHP binding. In the in vivo assay, we indirectly assessed the ability of SHP to interact with DNA-bound ER dimers. If SHP interacts, the VP16-SHP fusion protein should potentiate the ligand-dependent ER activation through the potent VP16 activation domain. For this purpose, we used VP16-SHPN1 (aa 37 to 260), which contains the central ER interaction domain (37) including NR box 2 of SHP and which interacted well in a mammalian two-hybrid assay with Gal4 fusions of both ERα and ERβ (data not shown). Increasing amounts of VP16-SHPN1 clearly enhanced the ligand-induced activity of both ERαwt (Fig. 7A) and ERβwt (Fig. 7B). The same effect could be seen with VP16-TIF2. However, a direct quantitative comparison of SHP- and TIF2-dependent interactions in this assay is complicated due to the possible contribution of the SHP repression domain in this transcription-based assay. Summarizing the results from these two independent interaction assays, we conclude that SHP binds to dimeric ERs via ternary complex formation. These interactions are consistent with NR box dependency and suggest that competition between SHP and TIF2 may occur directly on the AF-2 surface of DNA-bound ER dimers.

DISCUSSION

How SHP can regulate expression of target genes without the possibility to bind DNA directly has been the focus of research since its discovery (16, 35). Dissection of the mechanisms underlying the inhibitory effect of SHP on NR signaling requires a comprehensive understanding of the interaction of SHP with NRs. We show here that SHP binds directly to the AF-2 domain of ERs via two functional NR box motifs, and this finding may help to explain the unique interaction features of SHP, which previously have been difficult to understand assuming that SHP dimerizes with NRs (for a discussion, see reference 37). Thus, the ligand-dependent interactions, distinction between agonist and antagonist-bound ERs, requirement of the conserved AF-2 helix 12 within ERs, and nonrequire-

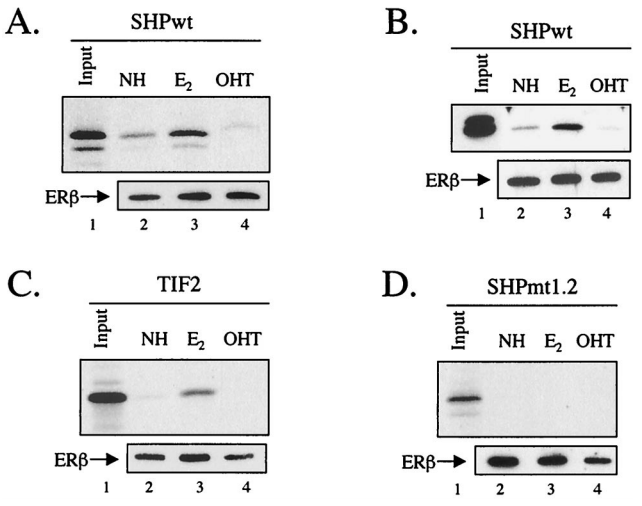

FIG. 6. SHPwt interacts with the DNA-bound ERβ in vitro. Binding of ^{35}S-labeled SHPwt (A), overexpressed SHPwt from Cos7 cells (B), ^{35}S-labeled TIF2 (aa 596 to 766) (C), or ^{35}S-labeled SHPmt1.2 (D) to ERβ assembled on a biotinylated ERE (from the vitelogenin A2 gene), in the absence or presence of 1 μM E_2 or 1 μM 4-OHT. The lower panel shows a Western analysis of the amount ERβ bound to ERE using a rabbit polyclonal antibody against hERβ.

ment of the putative dimerization helix 10 within SHP, all of which are characteristic for NR box-mediated cofactor interactions with the AF-2 domain, can now be understood due to the presence of NR box motifs within SHP.

Our data derived from studies of NR box core residue substitutions in the context of SHPwt are consistent with previous deletion studies indicating the requirement of a central interaction domain, SHP aa 92 to 148, for interactions with RXR and ER (36, 37). With the experimental demonstration that SHP NR box 2 is necessary and sufficient for ER interaction, we further delimited the minimal interaction domain to SHP aa 116 to 129. These experiments are significant for several reasons: first, the functional independency of the SHP box 2 motif confirms the NR box character of this motif; second, they substantially support our suggestion that competition between SHP and TIF2 occurs directly on the AF-2 surface (16); third, previous studies utilizing the SHP interaction domain have most likely characterized the NR box 2-mediated interactions of SHP with several NRs. Thus, many of the conclusions derived from our studies on ERs are likely to apply for other receptors as well.

Recent studies on LXXLL motifs have delineated several parameters which determine the binding specificity and affinity of cofactors to the AF-2 surface (7, 23, 32, 38). These include sequence variations within the core motif as well as within adjacent residues, variations in the number and the spacing of motifs within one molecule, and finally the secondary and structural context of the motif. To possibly understand the function of SHP NR boxes 1 and 2, as well as the nonfunctionality of SHP box 3, they should be discussed in light of these specific parameters.

Sequence requirements. SHP box 2 represents a novel variant of the NR box motif in that one of the core leucines at the +4 position is replaced by an isoleucine residue (LXXIL). This suggests that a certain variability of core residues may be tolerated for high-affinity ER binding. Indeed, in case of at least three AF-2 cofactors, namely, NSD1 (14), PSU1 (11), and RIP140 (13, 41), novel NR box variants have been identified which contain similar substitutions of the leucine residues. Intriguingly, both SHP and TIF2 motifs bound with apparently similar affinities to ERs in our two-hybrid measurements, further substantiating our suggestion that SHP competes with TIF2 (16). A direct comparison of the SHP and TIF2 motifs reveals additional similarities beyond the conserved leucine/isoleucine core (at positions +1, +3, and +4 [Fig. 3A]) that may dictate their high-affinity binding. These include a conserved isoleucine at position −1, which in the case of TIF2 box 2 makes direct contacts to ER AF-2 residues in the crystal structure and which is nonconserved in the two other TIF2 motifs (38), and also the conservation of positive charges (underlined) at positions +2 and +3 (TIF2-2, ILHRLL; SHP-2, ILKKIL). Although these residues do not directly contact the AF-2 residues, they may, in addition to adjacent residues, contribute to NR box specificity possibly through direct contacts to

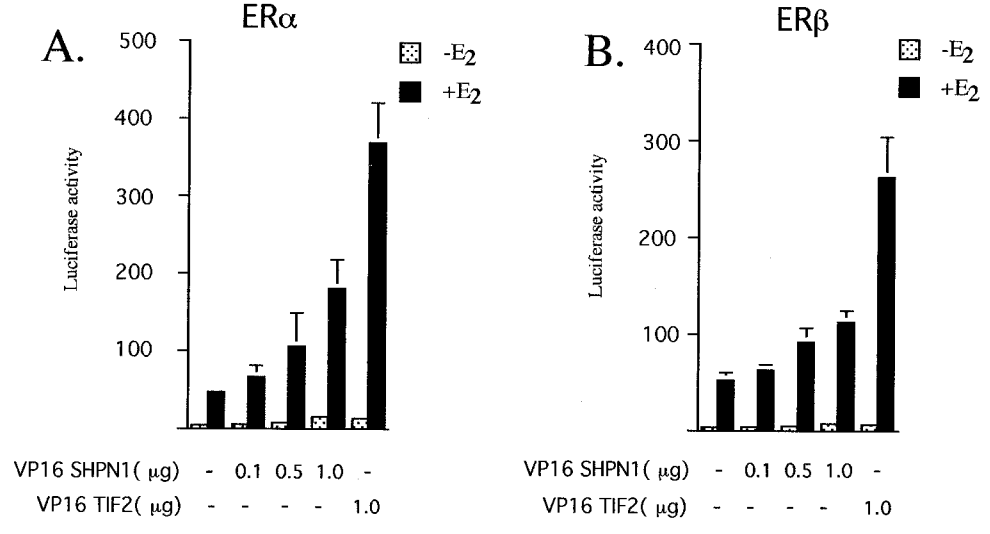

FIG. 7. Coexpression of VP16-SHP results in an enhanced ligand-mediated activation of ERs. 293 cells were cotransfected with the ERE-TATA-luc reporter plasmid and an expression plasmid for either ERαwt (A) or ERβwt (B) together with enhanced concentrations of VP16-SHPN1 (aa 37 to 260) or VP16-TIF2 (aa 596 to 766) in the absence or presence of 10 nM E_2. Values shown are the means of three independent experiments.

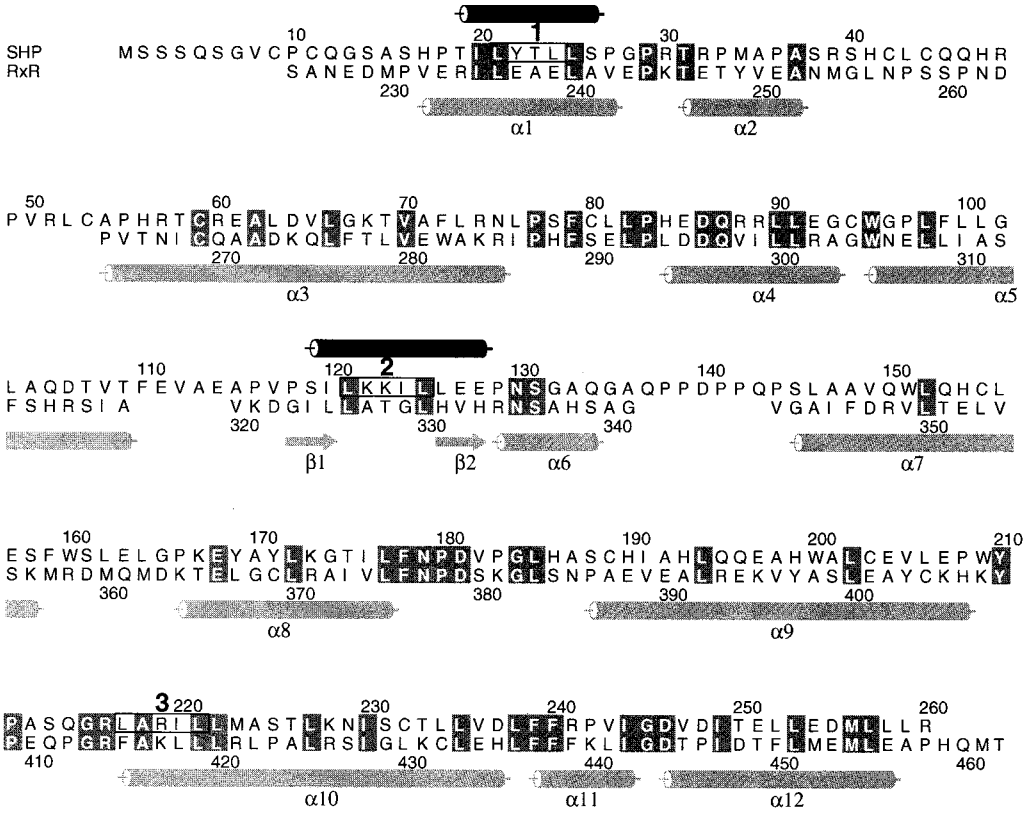

FIG. 8. Protein sequence alignment of rat SHP with human RXRα LBD. The alignment of secondary structure elements (below the sequence in grey) was derived from the three-dimensional structure of the RXRα apo-LBD (3). In case of SHP, the postulated localization of the NR box 1 and 2 α helices are shown (above the sequence in black). Identical residues are highlighted. Three LXXLL-related sequence motifs are boxed; motifs 1 and 2 corresponds to the functional SHP NR boxes 1 and 2, respectively; motif 3 corresponds to the nonfunctional NR box, that forms a part of the putative dimerization helix 10. For further explanations, see Discussion. The alignment was formatted using ALSCRIPT (2).

more distally located receptor domains (7, 23, 26). As with SHP box 2, the functional SHP box 1 is homologous to the TIF2 motif with regard to the leucine core (ILXXLL) but is nonconserved with regard to adjacent residues. In contrast, SHP box 3 differs from the two functional SHP NR boxes and the TIF2 box 2 in that it does not contain the critical isoleucine at the −1 position. In addition to its context (see below), this possibly accounts for the nonfunctionality of the SHP box 3 motif.

Number and spacing of motifs. The apparent functional redundancy of the two SHP motifs is reminiscent of the situation with AF-2 coactivators. As with other cofactors containing multiple NR boxes, the two SHP boxes may bind simultaneously but with distinct affinities to ERs and thus might exhibit different specificities to other receptor targets. With regard to spacing, the SHP boxes 1 and 2 are separated by at least 100 aa in primary structure, which is substantially different from the distance of adjacent NR boxes in p160 coactivators or in TRAP220/DRIP205 (reference 42 and references therein). However, they could be close to each other in the tertiary structure, considering the integration into an LBD. Thus, spacing may be context dependent (see below). Moreover, regarding stoichiometric considerations, receptor dimers may favor cofactors having multiple motifs (references 22 and 29 and references therein).

Structural context. Because SHP consists of a putative LBD, the internal localization of NR boxes raised the question of how functional independency can be accomplished within the compact LBD structure. Thus, the context may be more distinctive in SHP than in other NR box-containing cofactors. To understand the functionality of the NR boxes in the context of the entire SHP protein, we have aligned the SHP sequence to that of its closest relative, RXRα, for which the three-dimensional apo-LBD structure has been determined (3). Surprisingly, as our alignment indicates (Fig. 8), almost the entire SHP sequence matches the LBD fold. Therefore, we suggest that the SHP-specific N-terminal extension consists of only 20 residues, which is considerably shorter than originally anticipated (16, 35), and we believe it unlikely that the N terminus contains a DNA-binding function. Strikingly, the central interaction domain carrying the NR box 2 is found in exactly the region with the lowest sequence conservation between RXR and SHP. This region, located between helices 5 and 7, is not directly required for LBD stability and can vary in length between different LBDs (45). In RXR, this region is close to the surface of the LBD and encompasses the β-loop and the short helix 6. Alignments and structural predictions in this region are problematic in the case of SHP because of the lack of any sequence conservation and the presence of a 12-residue insertion. SHP shares this outstanding feature with its closest relative DAX-1, which carries an even longer insertion (26 residues) without predictable structure (19). Additionally, the proline environment juxtaposed to the NR box suggests unstructured regions, a proposed prerequisite for optimal AF-2 recognition and high-affinity binding. In the coactivator SRC-1, for example, short NR box helices are integrated into a largely

unstructured environment (for a discussion, see reference 29). Therefore, we suggest that significant structural differences exist within this SHP region, the major characteristics of which is the formation of the NR box 2 helix, perhaps integrated into an extended β loop and located at the surface of the LBD. Considering the functionality of unstructured NR box peptides prior to binding (7), it is relevant to speculate that α-helix formation may depend on interaction with the AF-2 target.

Surprisingly, with regard to SHP-box 1, our alignment suggests that it colocalizes precisely with the putative LBD helix 1. Critical leucines of the NR box 1 core and adjacent proline residues are not conserved in RXR or in any other NR, in agreement with their inability to mimic NR box-type interactions via helix 1. It is further tempting to speculate that the N-terminal localization in SHP, in contrast to the internality in other NRs, may allow a higher accessibility of this region for intermolecular interactions with target proteins. However, although helix 1 is not part of the LBD core, it contacts helices 3, 5, and 8 in other LBDs (45), and it is possible that such additional contacts may affect the functional independency of NR box 1. Indication for NR box 1 function also comes from the evolutionary conservation between rodent and human SHP proteins in the N terminus. Only the NR box 1/helix 1 region is identical in sequence, while the surrounding environment shows substantial sequence variation. Interestingly, SHP shares this feature with AF-2 cofactors such as p160 coactivators (for a discussion, see reference 21). In the case of SHP box 3, the colocalization with the putative dimerization helix 10 may explain its nonfunctionality as an NR box, in addition to its suboptimal sequence (as discussed above). Embedded into an extended helical region, this motif may not be available for high-affinity AF-2 binding. Furthermore, the lack of adjacent multiple proline residues distinguishes SHP box 3 from the two functional SHP NR boxes. Consistent with the similarity of the ER and RXR homodimer surface (45), SHP box 3-related motifs (underlined) can be found in helix 10 of ERs (RLAQLLL) and RXRs (RFAKLLL). Importantly, as seen in the crystal structures of the LBDs (3, 4, 38), not all three critical NR box core residues (positions +1, 3, and 4) are exposed to the surface, providing a possible explanation for why LXXLL-related motifs within the dimerization helix 10 cannot function as AF-2 binding motifs.

The distinctive role of NR boxes for SHP's interaction with ERs has functional implications for the inhibitory effects of SHP on NR activation. By combining the results from two different assays, we have been able to show that SHP indeed can bind to ER dimers on DNA, strongly arguing for the formation of ternary or higher-order complexes. Notably, in these experiments SHP interacted with ER in the same way as the coactivator TIF2 did, suggesting that competition between coactivators and SHP (16) may occur also on DNA-bound receptors. Additionally, by showing that an NR box-containing but repression-defective SHP derivative (aa 1 to 159) (37) is no longer able to inhibit ER activation, it is likely that active repression mechanisms contribute to SHP's inhibitory function in vivo. SHP may function in a two-step mechanism: first, binding to the AF-2 domain, which may include either prevention of coactivator binding or displacement of prebound coactivators; second, recruitment of corepressors via its own LBD. Although the precise repression mechanisms including SHP-associated corepressors have not been identified, the exciting possibility exists that SHP might bridge ligand-activated receptors to corepressor complexes, and SHP thus may define a novel category of corepressors.

Considering that natural hormones and synthetic agonistic ligands usually positively regulate target genes via AF-2 activation of their target receptors, it is relevant to ask why evolution has added SHP-like corepressors to the large number of AF-2 coactivators. The question is further relevant because additional NR box-containing AF-2 cofactors exist that exhibit negative-regulatory or repressive functions. Such cofactors include possibly RIP140, TIF1, NSD1 (27), and the SHP relative DAX-1 (see below). (i) We suggest that SHP may play a central role in regulation of NR-coactivator interactions. Since almost all relevant coactivators bind via LXXLL motifs to the AF-2 domain, different SHP levels may introduce subtle variations in the coactivator subunit composition that, in turn, may generate receptor-, ligand-, or tissue-specific complexes. This possibility is in line with current suggestions that similar competitive interactions are necessary to establish sequential cascades in coactivator recruitment and may further allow the generation of tissue- or cell-specific coactivator complexes (for a discussion, see reference 10). (ii) SHP may be involved in attenuation and feedback control of hormone-regulated gene expression (reference 6 and references therein), possibly by including (ligand-)regulated changes in SHP's binding affinity or local nuclear concentration. (iii) Considering the location of the functional SHP NR box 2 within the putative LBD, it is tempting to speculate that unidentified SHP ligands (i.e., agonists or antagonists) could induce conformational changes which in turn may affect SHP's NR box-mediated interactions with NRs positively or negatively, offering yet another exciting possibility for the putative regulatory impact of SHP on NR signaling. (iv) Ligand binding could convert SHP from a repressor to an activator by recruitment of novel coactivators to SHP. In such a situation, SHP would be able to transmit its own ligand signaling to, for example, estrogen target genes. Intriguingly, SHP may share this feature with its closest relative within the NR superfamily, the orphan receptor DAX-1, which also lacks an NR-typical DBD but, unlike SHP, instead utilizes a novel three-repeat domain for DNA binding and for direct interaction with the orphan receptor SF-1. Indeed, we have noticed the presence of conserved NR box-like motifs in the DAX-1 three-repeat region. Finally, it is remarkable from the evolutionary point of view that SHP, a unique LBD-only member of the NR superfamily, has acquired this cofactor function, which is mechanistically different from conventional dimerization-type interactions of NRs. SHP's potential to silence or redirect ligand signaling provides a novel and unique mechanism of cross-talk between NRs and places SHP structurally and functionally between NRs and their associated transcriptional cofactors.

ACKNOWLEDGMENTS

A. Båvner and J. S. Thomsen contributed equally to this work.

We thank M. G. Parker, P. Kushner, J. Leers, J. Zilliacus, and D. P. McDonnell for providing plasmids. We are also grateful to members of the Unit for Receptor Biology at Novum for providing materials and fruitful discussions.

This work was supported by KaroBio AB and the Swedish Cancer Society.

REFERENCES

1. **Anonymous.** 1999. A unified nomenclature system for the nuclear receptor superfamily. Cell **97:**161–163.
2. **Barton, G. J.** 1993. ALSCRIPT: a tool to format multiple sequence alignments. Protein Eng. **6:**37–40.
3. **Bourguet, W., M. Ruff, P. Chambon, H. Gronemeyer, and D. Moras.** 1995. Crystal structure of the ligand-binding domain of the human nuclear receptor RXR-alpha. Nature **375:**377–382.
4. **Brzozowski, A. M., A. C. Pike, Z. Dauter, R. E. Hubbard, T. Bonn, O. Engstrom, L. Ohman, G. L. Greene, J. Å. Gustafsson, and M. Carlquist.** 1997. Molecular basis of agonism and antagonism in the estrogen receptor. Nature **389:**753–758.

5. **Cavailles, V., S. Dauvois, P. S. Danielian, and M. G. Parker.** 1994. Interaction of proteins with transcriptionally active estrogen receptors. Proc. Natl. Acad. Sci. USA **91:**10009–10013.
6. **Chen, H., R. J. Lin, W. Xie, D. Wilpitz, and R. Evans.** 1999. Regulation of hormone-induced histone hyperacetylation and gene activation via acetylation of an acetylase. Cell **98:**675–686.
7. **Darimont, B. D., R. L. Wagner, J. W. Apriletti, M. R. Stallcup, P. J. B. Kushner, J. D., R. J. Fletterick, and K. R. Yamamoto.** 1998. Structure and specificity of nuclear receptor-coactivator interactions. Genes Dev. **12:**3343–3356.
8. **Ding, X. F., C. M. Anderson, H. Ma, H. Hong, R. M. Uht, P. J. Kushner, and M. R. Stallcup.** 1998. Nuclear receptor-binding sites of coactivators glucocorticoid receptor interacting protein 1 (GRIP1) and steroid receptor coactivator 1 (SRC- 1): multiple motifs with different binding specificities. Mol. Endocrinol. **12:**302–313.
9. **Enmark, E., and J. Å. Gustafsson.** 1996. Orphan nuclear receptors—the first eight years. Mol. Endocrinol. **10:**1293–1307.
10. **Freedman, L.** 1999. Increasing the complexity of coactivation in nuclear receptor signaling. Cell **97:**5–8.
11. **Gaudon, C., P. Chambon, and R. Losson.** 1999. Role of the essential yeast protein PSU1 in transcriptional enhancement by the ligand-dependent activation function AF-2 of nuclear receptors. EMBO J. **18:**2229–2240.
12. **Glass, C. K., D. W. Rose, and M. G. Rosenfeld.** 1997. Nuclear receptor coactivators. Curr. Opin. Cell Biol. **9:**222–232.
13. **Heery, D. M., E. Kalkhoven, S. Hoare, and M. G. Parker.** 1997. A signature motif in transcriptional co-activators mediates binding to nuclear receptors. Nature **387:**733–736.
14. **Huang, N., E. vom Baur, J. M. Garnier, T. Lerouge, J. L. Vonesch, Y. Lutz, P. Chambon, and R. Losson.** 1998. Two distinct nuclear receptor interaction domains in NSD1, a novel SET protein that exhibits characteristics of both corepressors and coactivators. EMBO J. **17:**3398–3412.
15. **Ito, M., C. X. Yuan, S. Malik, W. Gu, J. D. Fondell, S. Yamamura, Z. Y. Fu, X. L. Zhang, J. Qin, and R. G. Roeder.** 1999. Identity between TRAP and SMCC complexes indicates novel pathways for the function of nuclear receptors and diverse mammalian activators. Mol. Cell **3:**361–370.
16. **Johansson, L., J. S. Thomsen, A. E. Damdimopoulos, G. Spyrou, J. Å. Gustafsson, and E. Treuter.** 1999. The orphan nuclear receptor SHP inhibits agonist-dependent transcriptional activity of estrogen receptors ER-alpha and ER-beta. J. Biol. Chem. **274:**345–353.
17. **Kalkhofen, E., J. E. Valentine, D. M. Heery, and M. G. Parker.** 1998. Isoforms of steroid receptor co-activator 1 differ in their ability to potentiate transcription by the oestrogen receptor. EMBO J. **17:**232–243.
18. **Kurokawa, R., M. Söderström, A. Hörlein, S. Halachmi, M. Brown, M. G. Rosenfeld, and C. K. Glass.** 1995. Polarity-specific activities of retinoic acid receptors determined by a co-repressor. Nature **377:**451–454.
19. **Lalli, E., B. Bardoni, E. Zazopoulos, J. M. Wurtz, T. M. Strom, D. Moras, and P. Sassone-Corsi.** 1997. A transcriptional silencing domain in DAX-1 whose mutation causes adrenal hypoplasia congenita. Mol. Endocrinol. **11:**1950–1960.
20. **Le Douarin, B., A. L. Nielsen, J. M. Garnier, H. Ichinose, F. Jeanmougin, R. Losson, and P. Chambon.** 1996. A possible involvement of TIF1 alpha and TIF1 beta in the epigenetic control of transcription by nuclear receptors. EMBO J. **15:**6701–6715.
21. **Leers, J., E. Treuter, and J. Å. Gustafsson.** 1998. Mechanistic principles in NR box-dependent interaction between nuclear hormone receptors and the coactivator TIF2. Mol. Cell. Biol. **18:**6001–6013.
22. **L'Horset, F., S. Dauvois, D. M. Heery, V. Cavailles, and M. G. Parker.** 1996. RIP-140 interacts with multiple nuclear receptors by means of two distinct sites. Mol. Cell. Biol. **16:**6029–6036.
23. **Mak, H. Y., S. Hoare, P. M. Henttu, and M. G. Parker.** 1999. Molecular determinants of the estrogen receptor-coactivator interface. Mol. Cell. Biol. **19:**3895–3903.
24. **Mangelsdorf, D. J., and R. M. Evans.** 1995. The RXR heterodimers and orphan receptors. Cell **83:**841–850.
25. **Masuda, N., H. Yasumo, T. Tamura, N. Hashiguchi, T. Furusawa, T. Tsukamoto, H. Sadano, and T. Osumi.** 1997. An orphan nuclear receptor lacking a zinc-finger DNA-binding domain: interaction with several nuclear receptors. Biochim. Biophys. Acta **1350:**27–32.
26. **McInerney, E. M., D. W. Rose, S. E. Flynn, S. Westin, T. M. Mullen, A. Krones, J. Inostroza, J. Torchia, R. T. Nolte, N. Assa-Munt, M. V. Milburn, C. K. Glass, and M. G. Rosenfeld.** 1998. Determinants of coactivator LXXLL motif specificity in nuclear receptor transcriptional activation. Genes Dev. **12:**3357–3368.
27. **McKenna, N. J., R. B. Lanz, and B. W. O'Malley.** 1999. Nuclear receptor coregulators: cellular and molecular biology. Endocrine Rev. **20:**321–344.
28. **Nishikawa, J., K. Saito, J. Goto, F. Dakeyama, M. Matsuo, and T. Nishihara.** 1999. New screening methods for chemicals with hormonal activities using interaction of nuclear receptor with coactivator. Toxicol. Appl. Pharmacol. **154:**76–83.
29. **Nolte, R. T., G. B. Wisely, S. Westin, J. E. Cobb, M. H. Lambert, R. Kurokawa, M. G. Rosenfeld, T. M. Willson, C. K. Glass, and M. V. Milburn.** 1998. Ligand binding and co-activator assembly of the peroxisome proliferator-activated receptor gamma. Nature **395:**137–143.
30. **Norris, J. D., D. Fan, M. R. Stallcup, and D. P. McDonnell.** 1998. Enhancement of estrogen receptor transcriptional activity by the coactivator GRIP-1 highlights the role of activation function 2 in the determining estrogen receptor pharmacology. J. Biol. Chem. **273:**6679–6688.
31. **Paech, K., P. Webb, G. G. Kuiper, S. Nilsson, J. Gustafsson, P. J. Kushner, and T. S. Scanlan.** 1997. Differential ligand activation of estrogen receptors ERalpha and ERbeta at AP1 sites. Science **277:**1508–1510.
32. **Paige, L. A., D. J. Christensen, H. Gron, J. D. Norris, E. B. Gottlin, K. M. Padilla, C. Y. Chang, L. M. Ballas, P. T. Hamilton, D. P. McDonnell, and D. M. Fowlkes.** 1999. Estrogen receptor (ER) modulators each induce distinct conformational changes in ER alpha and ER beta. Proc. Natl. Acad. Sci. USA **96:**3999–4004.
33. **Puigserver, P., Z. Wu, C. W. Park, R. Graves, M. Wright, and B. M. Spiegelman.** 1998. A cold-inducible coactivator of nuclear receptors linked to adaptive thermogenesis. Cell **92:**829–839.
34. **Rachez, C., Z. Suldan, J. Ward, C. P. Chang, D. Burakov, H. Erdjument-Bromage, P. Tempst, and L. P. Freedman.** 1998. A novel protein complex that interacts with the vitamin D3 receptor in a ligand-dependent manner and enhances VDR transactivation in a cell-free system. Genes Dev. **12:**1787–1800.
35. **Seol, W., H. S. Choi, and D. D. Moore.** 1996. An orphan nuclear hormone receptor that lacks a DNA binding domain and heterodimerizes with other receptors. Science **272:**1336–1339.
36. **Seol, W., M. Chung, and D. D. Moore.** 1997. Novel receptor interaction and repression domains in the orphan receptor SHP. Mol. Cell. Biol. **17:**7126–7131.
37. **Seol, W., B. Hanstein, M. Brown, and D. D. Moore.** 1998. Inhibition of estrogen receptor action by the orphan receptor SHP (short heterodimer partner). Mol. Endocrinol. **12:**1551–1557.
38. **Shiau, A. K., D. Barstad, P. M. Loria, L. Cheng, P. J. Kushner, D. A. Agard, and G. L. Greene.** 1998. The structural basis of estrogen receptor/coactivator recognition and the antagonism of this interaction by tamoxifen. Cell **95:**927–937.
39. **Struhl, K.** 1998. Histone acetylation and transcriptional regulatory mechanisms. Genes Dev. **12:**599–606.
40. **Torchia, J., D. W. Rose, J. Inostroza, Y. Kamei, S. Westin, C. K. Glass, and M. G. Rosenfeld.** 1997. The transcriptional co-activator p/CIP binds CBP and mediates nuclear-receptor function. Nature **387:**677–684.
41. **Treuter, E., T. Albrektsen, L. Johansson, J. Leers, and J. Å. Gustafsson.** 1998. A regulatory role for RIP140 in nuclear receptor activation. Mol. Endocrinol. **12:**864–881.
42. **Treuter, E., L. Johansson, J. S. Thomsen, A. Wärnmark, J. Leers, M. Pelto-Huikko, M. Sjöberg, A. P. H. Wright, G. Spyrou, and J. Å. Gustafsson.** 1999. Competition between TRAP220 and TIF2 for binding to nuclear receptors. J. Biol. Chem. **274:**6667–6677.
43. **Voegel, J. J., M. J. Heine, M. Tini, V. Vivat, P. Chambon, and H. Gronemeyer.** 1998. The coactivator TIF2 contains three nuclear receptor-binding motifs and mediates transactivation through CBP binding-dependent and -independent pathways. EMBO J. **17:**507–519.
44. **Westin, S., R. Kurokawa, R. T. Nolte, G. B. Wisely, E. M. McInerney, D. W. Rose, M. V. Milburn, M. G. Rosenfeld, and C. K. Glass.** 1998. Interactions controlling the assembly of nuclear-receptor heterodimers and co-activators. Nature **395:**199–202.
45. **Wurtz, J. M., W. Bourguet, J. P. Renaud, V. Vivat, P. Chambon, D. Moras, and H. Gronemeyer.** 1996. A canonical structure for the ligand-binding domain of nuclear receptors. Nat. Struct. Biol. **3:**87–94.
46. **Zhou, G., R. Cummings, Y. Li, S. Mitra, H. A. Wilkinson, A. Elbrecht, J. D. Hermes, J. M. Schaeffer, R. G. Smith, and D. E. Moller.** 1998. Nuclear receptors have distinct affinities for coactivators: characterization by fluorescence resonance energy transfer. Mol. Endocrinol. **12:**1594–1604.